Cancer Chemother Pharmacol (2006) 57: 761–771
DOI 10.1007/s00280-005-0120-6

ORIGINAL ARTICLE

**Lucy Lee · Sunil Sharma · Bruno Morgan
Peter Allegrini · Christian Schnell · Josef Brueggen
Robert Cozens · Mark Horsfield · Clemens Guenther
Will P. Steward · Joachim Drevs · David Lebwohl
Jeanette Wood · Paul M. J. McSheehy**

# Biomarkers for assessment of pharmacologic activity for a vascular endothelial growth factor (VEGF) receptor inhibitor, PTK787/ZK 222584 (PTK/ZK): translation of biological activity in a mouse melanoma metastasis model to phase I studies in patients with advanced colorectal cancer with liver metastases

Received: 21 May 2005 / Accepted: 19 August 2005 / Published online: 20 September 2005


**Abstract** PTK/ZK is a novel, oral angiogenesis inhibitor that specifically targets all 3 vascular endothelial growth factor (VEGF) receptor tyrosine kinases and is currently in phase III clinical trials. In early clinical trials, PTK/ZK demonstrated a dose-dependent reduction in tumor vascular parameters as measured by dynamic contrast-enhanced magnetic resonance imaging (DCE-MRI) and an acute increase in plasma VEGF levels. The reduction in tumor vascularity was significantly correlated with improved clinical outcome in patients with advanced colorectal cancer and liver metastases. To assess the predictive value of a mouse model of tumor metastases, comparisons were performed for the biological activity of PTK/ZK in the mouse model and in patients with liver metastases in the clinical phase I trials. An orthotopic, syngeneic mouse model was used: C57BL/6 mice injected in the ear with murine B16/BL6 melanoma cells which metastases to the cervical lymph-nodes. The primary tumor and spontaneous metastases express VEGF and VEGF receptors and respond to treatment with VEGFR tyrosine kinase inhibitors. PTK/ZK was administered orally, with assesments by DCE-MRI of the metastases and plasma VEGF taken predose and at 3 days posttreatment and efficacy determined at 7 days posttreatment. Dose-ranging studies in naive mice provided preclinical pharmacokinetic data, while two dose-escalation phase I studies provided clinical pharmacokinetic data. An exposure–response relationship was observed both for mouse metastases (measured as % tumor weight treated/control) and for human liver metastases (measured as % regression). In the B16/BL6 model, the active dose of 50 mg/kg PTK/ZK yielded 62.4 (± 16.0) h μM plasma exposure, which is comparable to the plasma area under the concentration time curve (AUC) achieved by the 1000 mg dose of PTK/ZK used in clinical trials. At this exposure level in clinical trials, DCE-MRI showed a reduction in the area under the enhancement curve (IAUC) to 47% of baseline. At a similar exposure in the PTK/ZK-treated mice, a reduction in IAUC to 75% of baseline was observed. Furthermore, at doses of 50 mg/kg PTK/ZK and above, an increase in plasma VEGF level 10 h after drug administration was observed in mice which was consistent with findings from the clinical trials. In conclusion, the preclinical pharmacodynamics of PTK/ZK correlate well with clinical activity in phase I trials over comparable exposures to the drug. Thus, data

L. Lee (✉) · S. Sharma · D. Lebwohl
Translational and Clinical Development, Oncology Business Unit, Novartis Pharmaceutical, One Health Plaza Bldg 105, East Hanover, NJ 07936, USA
E-mail: lucy.lee@novartis.com
Tel.: +1-862-7784180
Fax: +1-973-7816598

B. Morgan · M. Horsfield · W. P. Steward
University of Leceister, Leicester, UK

P. Allegrini · C. Schnell · J. Brueggen · R. Cozens
J. Wood · P. M. J. McSheehy
Oncology Research, Novartis Institute of Biomedical Research, Basel, Switzerland

C. Guenther
Clinical Development, Schering AG, Berlin, Germany

J. Drevs
Tumor Biology, Freiburg, Germany

from this preclinical model proved to be consistent with and thus predictive of the biologic effects of PTK/ZK in phase I/II clinical trials.

**Keywords** Angiogenesis · VEGF · VEGF receptor inhibitor · Interspecies scaling · Pharmacokinetic

## Introduction

Contemporary approaches to drug development are target-based, with the target being the one that is implicated in the molecular or cellular pathology of cancer. Specifically, in vivo models in the development of signal transduction modifiers and tumor angiogenesis inhibitors are used to demonstrate the fact that the required drug-target interaction takes place, and that interaction leads to the desired downstream biological effects. Increasingly, such biological effects are not measured as tumor regression, but are assessed using pharmacodynamic assays or biomarkers. As such, validated in vivo models and proven biological markers for drug effects are two important components in preclinical and early clinical drug development that will allow for an accelerated selection of successful drug candidates as well as an expedited identification of the clinically active dose.

PTK787/ZK 222584 (PTK/ZK), generic name vatalanib, is an orally active angiogenesis inhibitor blocking all known vascular endothelial growth factor receptors (VEGF-R) with slightly greater potency against the VEGF-R1 and VEGF-R2 [1–3]. It is approximately sevenfold less active against the mouse receptor than against the equivalent human receptor. The in vitro IC50s (uM) for the isolated protein kinases are the following: 0.037 (VEGF-R2, KDR, human), 0.077 (VEGF-R1, Flt-1, human), 0.271 (VEGF-R2, Flk, mouse), 0.660 (VEGF-R3, Flt-4), and 0.580 (PDGF-R). PTK/ZK demonstrated dose-dependent inhibition of VEGF-induced proliferation of human umbilical vein endothelial cells with an IC50 of 0.007 μM, and in vivo, primarily reduced the number of immature tumor microvessels accompanied by hemodynamic dilation of the remaining vessels [3, 4].

Recently, dynamic contrast-enhanced magnetic imaging (DCE-MRI), which measures vascular perfusion and permeability characteristics of tumors, was established as a clinical biomarker for early assessment of antiangiogenic activities in patients with colorectal cancer and liver metastases [5]. An integrated assessment of exposure–response relationships was performed using pharmacokinetic, pharmacodynamic (as assessed by DCE-MRI), and tumor response data from two phase I trials. The findings demonstrated a strong correlation between PTK/ZK exposure and changes in tumor vascularity measured by DCE-MRI, and further showed that DCE-MRI was a strong predictor of tumor response. The selected biologically active dose, under evaluation in phase III trials to confirm efficacy in patients with colorectal cancer and liver metastases, was chosen based upon achieving a plasma area-under-the-concentration-time-curve (AUC) for PTK/ZK that was associated with a threshold DCE-MRI effect for non-progressive disease.

The discovery of DCE-MRI as a "biomarker" for assessment of antiangiogenic activity has generated much interest in both the preclinical as well as the clinical community. DCE-MRI is currently being used to profile compounds for activities in preclinical research; however, a formal analysis to compare the relationship between preclinical results to the clinical findings has not been well documented. Therefore, the purpose of this investigation was to assess retrospectively, whether the results of PTK/ZK treatment in a mouse B16/BL6 metastatic tumor model could be translated to the findings in the two clinical phase I trials. Supportive comparative analysis for efficacy and other markers of antiangiogenesis, i.e. plasma VEGF, were also performed.

A preclinical model of colorectal liver metastasis was not available; however, the B16/BL6 melanoma model is an orthotopic and syngeneic mouse model where spontaneous metastases form in the cervical lymph-nodes from the primary tumor growing from cells implanted intradermally in the skin of the ear. The metastases express VEGF and VEGFR [6] and respond to treatment with VEGFR tyrosine kinase inhibitors. Because the B16/BL6 metastases are highly vascularized, they provide an excellent signal for DCE-MRI assessment. In this investigation, the pharmacodynamic effects achieved across a range of equivalent PTK/ZK exposures in mice bearing B16/BL6 melanoma and in patients from Phase I clinical trials were compared to determine whether the preclinical model is predictive of clinical response. In PTK/ZK treated mice, the findings showed that the maximum antitumor activity and effects on DCE-MRI were observed at PTK/ZK exposures which correspond to the exposure achieved by the selected clinically active dose for evaluation in Phase III trials.

## Method

### Clinical studies

#### *Phase I studies*

The patients, included in this analysis, were with histologically confirmed advanced colorectal cancer with liver metastases from two phase I dose escalation studies at centers involving the oncology and radiology departments at Leicester, UK (Study 0101) and Freiburg, Germany (Study 0101 and 0103). PTK/ZK was administered orally on a continuous-once daily schedule on 28-day cycles until patient discontinued from study due to intolerable toxicity or tumor progression. The starting

dose was based on preclinical toxicity data with the subsequent dose escalation levels using an approximated Fibonacci Series: 50, 150, 300, 500, 750, 1000, 1200, 1500, and 2000 mg.

### *Pharmacokinetic assessments*

Full pharmacokinetic samples were obtained on days 1, 15, and 28 in the first cycle of therapy at the following time points: predose (0), 0.25, 0.5, 1, 1.5, 2, 4, 6, 10, and 24 h postdose. Using a noncompartmental method (WinNonlin Pro 3.2, Pharsight Corp), $AUC_{0-\infty}$was calculated on day 1 using the linear trapezoidal rule up to the last measurable data point, and then extrapolated to infinity. $AUC_{0-24}$ was calculated on day 28 using the linear trapezoidal rule up to 24 h postdose.

### *DCE-MRI assessments*

DCE-MRI imaging was performed at baseline (within 1 week prior to treatment with PTK/ZK), on day 2 and on day 28 and 56. Posttreatment effects (expressed as % of baseline) were assessed on day 2, 28 and 56. Tumor permeability and vascularity were assessed by calculating the bi-directional transfer constant ($K_i$) and the area under the enhancement curve (IAUC) over 4.5 min. This IAUC is equivalent to that measured and defined in the animal model (see below). A review of the literature shows that % changes in $K_i$ and IAUC are broadly correlated [6, 7, 8].

### *Plasma markers of angiogenesis assessments*

Plasma and serum samples were obtained for markers of angiogenesis and activated endothelial cells (VEGF, bFGF, sTIE-2, sE-SEL) in every treatment cycle. All samples were collected at baseline and at time points immediately before dosing on days 1, 8, 15, 22, and 28. All data were expressed as % of baseline, and the average of % of baseline were used in the assessment for posttreatment effects.

### *Tumor size assessment*

Patients were evaluated for tumor response at the end of every 28-day cycle using the solid tumor response criteria (SWOG) [9]. All measurable, evaluable, and nonevaluable lesions were accounted for in the tumor assessment, with measurable lesions quantified by using the product of perpendicular diameters. The best tumor response was defined based on the sequence of tumor response at the end of the first and/or second cycle of treatment. The categories for best tumor response are as follows: ''Progressive'' (P): patients who progressed within the first two cycles of treatment; ''Nonprogressive'' (NP): patients who maintained stable disease for the first two cycles of treatment; and ''Not evaluable'' (NE): patients who did not have sufficient tumor response data to be categorized as P or NP. The change in the size of the measured lesions (expressed as % of baseline) at the end of cycle 1 or 2 were included in the efficacy analysis.

The complete details of the clinical trials and DCE-MRI methodology and soluble marker bioanalytical assays are described in Morgan et al. [5] and Drevs et al. [10].

## Preclinical studies

### *Animal model*

Female C57BL/6 mice were used for all experiments. Murine B16/BL6 melanoma cells were originally obtained from Prof IJ. Fidler, (MD Anderson Cancer Centre, Texas, USA). B16/BL6 cells were injected intradermally in both ears of the mice as described previously [6]. The primary tumors are clearly visible within 7 days and metastasize rapidly to the cervical (neck) lymph-nodes which are palpable by day 14. All experiments were started at approximately 14 days after cell inoculation. For this analysis, only the cervical lymph-node metastases were studied for the effects of PTK/ZK on tumor size and tumor vascularity/perfusion as measured by DCE-MRI.

### *Pharmacokinetic assessments*

Plasma samples for measurement of drug concentrations were obtained after single PTK/ZK administration (doses: 10, 50, and 200 mg/kg, p.o., 3 to 4 mice per dose group) to the tumor-bearing mice at the following time points: predose (0), 0.5, 2, 6, 10, and 24 h postdose. Concentrations of PTK/ZK were measured by HPLC as described previously [1]. Using a noncompartmental method (WinNonlin Pro 3.2, Pharsight Corp), $AUC_{0-\infty}$was calculated on day 1 using the linear trapezoidal rule up to the last measurable data point, and then extrapolated to infinity. Full pharmacokinetic samples at the highest tolerable doses were also obtained in naïve mice, rat, and dog for the purpose of allometric scaling. Compartmental methods were used to estimate the pharmacokinetic parameters.

### *DCE-MRI assessments*

Tumor vascularity/perfusion was assessed by DCE-MRI following bolus i.v. injection of the contrast agent GdDOTA (Dotarem, 0.1 mmoles/kg) on day 0 (baseline) and day 3 posttreatment and the effect expressed as % of baseline as previously described [6, 11]. Parameters for MRI include vascular permeability (VP), i.e., the initial slope for GdDOTA uptake, interstitial leakage

space (LS), i.e., the plateau for GdDOTA, and the initial IAUC from time 0 to 102 s which is related to VP and LS and is equivalent to the IAUC measured in the clinic [6]. Only data for the IAUC is presented. In addition, in the same animals, tumor uptake of Endorem (Feridex, Guerbet Laboratories), a large molecule supraparamagnetic iron oxide MRI contrast agent, was measured, providing a measure of blood flow index (BFI) and relative blood volume (rBVol) [6, 11]. Selected doses were also based on prior pharmacology [1] and toxicology experiments with at least 4 mice per dose group: 0, 3, 30, 50, 100, and 200 mg/kg, p.o. on a daily schedule. There were some dropouts with the highest dose due to technical failures, so data for the 200 mg/kg dose is not shown.

### *Plasma markers of angiogenesis assessments*

Plasma samples were taken from several mice at different time points: 0.5, 2, 6 and 10 h post a single treatment with PTK787 (0, 10, 50 and 200 mg/kg p.o.) from mice bearing established metastases (14 day post cell inoculation in the ear). Samples were collected in separation tubes, allowed to stand at room temperature for 90 s and then spun at 4°C for 7 min at 7000 rpm (Sigma MK). The supernatant was taken and tested immediately. VEGF concentration was measured using an ELISA assay kit for murine VEGF (R & D Systems, London, UK).

### *Tumor size assessment*

Tumor size measurements were performed on day 7 posttreatment by removal of the metastases and comparison of the final weight with the vehicle treatment group (expressed as %T/C). Selected doses were based on prior pharmacology and toxicology experiments with 4 to 6 mice per dose group: 3, 30, 100, and 200 mg/kg administered, p.o. on a daily schedule.

### Preclinical and clinical data analysis: comparison and correlation

Previously, it was shown that a mathematical model, such as an inhibitory $E_{max}$ model, best characterizes the relationship between biomarker effect of the drug using MRI $K_i$ and the drug exposure [5]. In the current analysis, the same modeling was attempted for MRI and efficacy for both preclinical and clinical data. An MRI-derived parameter, the initial IAUC from contrast injection to a time 270 s later, was used instead of $K_i$ since this could be calculated for both preclinical and clinical data. To accommodate a limited number of data points, the MRI IAUC data from day 2 and day 28 (EC1 = end of cycle 1) were pooled in the modeling. For efficacy assessment, %T/C was used for preclinical data and % of baseline measured tumor size was used for clinical data.

$$\text{Effect} = E_0 - (E_0 - E_{\max}) \times \left(\frac{\text{AUC}}{\text{AUC} + \text{E}_{AUC50}}\right)$$

where Effect is MRI IAUC or efficacy achieved with PTK/ZK AUC, $E_0$ is baseline MRI IAUC OR efficacy (~100%), $E_{AUC50}$ is PTK/ZK AUC in which 50% of $E_{max}$ is achieved, $E_{max}$ is maximum MRI IAUC or efficacy. *AUC in equation denotes PTK/ZK AUC.

Parameters were estimated using the Nelder Mead Simplex [12] algorithm and a weighting scheme was used, if appropriate. The $E_0$ parameter was fixed at approximately 100% due to high variability in MRI as it approaches 100%. The final model was selected based on a battery of diagnostic tests, including graphical evaluation of the residual plots and comparison of Akaike [13] and Schwarz [14] criteria.

As the intent of this evaluation was to assess how well the preclinical data translates to the clinical data, the preclinical data was used to predict a theoretical clinical PK-PD, and this was compared to the observed clinical PK-PD data. The predicted clinical PK-PD data was simulated using modeled preclinical parameters which were "scaled-up" to approximate clinical parameters. Preclinical PK parameters were scaled-up using allometric methods, where clearance (Cl) and volume of distribution (V) were predicted using the equation expressed below. This variation of the allometric method, incorporating brain weight (BW), was selected based on initial evaluation of the preclinical data obtained from the mice, rat, and dog [15, 16]

$$PK \text{ parameter} * BW = a(W)^b$$

where $PK$ parameter is Cl or V , $BW$ is brain weight (kg), $W$ is body weight (kg), $a$is allometric coefficient of equation, $b$ is allometric exponent of equation.

The absorption rate constant (ka) was estimated from rat data, as physiological properties in this species were found to best correlated to man [17]. Using the scaled PK-PD parameters, a range of AUCs were simulated for single clinical doses (50–2000 mg). Thereafter, the MRI effects for the range of AUCs were simulated using the PK-PD model. Graphical comparisons for the predicted and observed MRI effects in human were performed over the entire PTK/ZK exposure range. No formal inferential statistics was performed. In addition, comparison of changes in plasma VEGF levels with PTK/ZK treatment between that of the animal and man were graphically performed.

## Results

### Clinical studies

The dose-PTK/ZK exposure (day 28) relationship is shown in Fig. 1 (top) and the PTK/ZK exposures (days 1

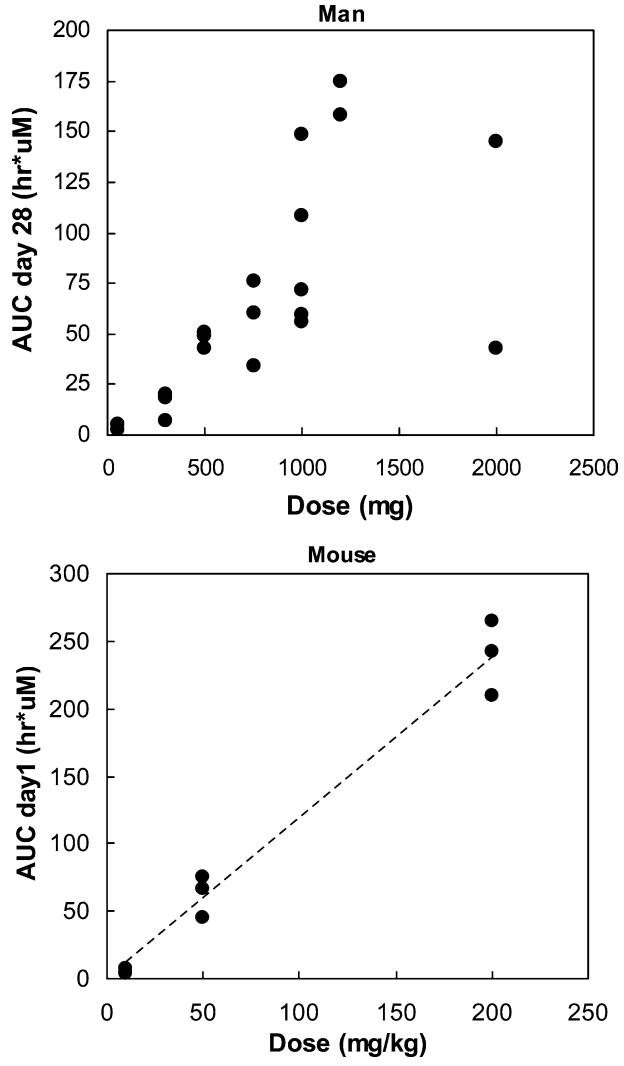


**Fig. 1** Dose versus plasma AUC for PTK/ZK in man on day 28 (top) and in mouse on day 1 (bottom) with linear regression

**Table 1** Mean ± (SD) plasma AUC for PTK/ZK in man after single and multiple doses

| Dose (mg/day) $N$ = (day 1/day 28) | Pharmacokinetic parameter | |
|---|---|---|
| | $AUC_{0-\infty}$ (day 1) | $AUC_{0-24}$ (day 28) |
| 50 (2/2) | 3.1 ± 2.49 | 4.22 ± 1.67 |
| 300 (3/3) | 15.19 ± 6.94 | 14.97 ± 6.99 |
| 500 (3/3) | 73.69 + 29.44 | 47.50 ± 3.93 |
| 750 (3/3) | 94.28 ± 83.66 | 56.97 ± 21.24 |
| 1000 (5/5) | 241.10 ± 89.84 | 88.67 ± 39.12 |
| 1200 (6/2) | 250.1 ± 161.5 | 166.3 ± 11.59 |
| 1500 (1/0) | 126.5 | – |
| 2000 (3/2) | 204.9 ± 118.8 | 93.9 ± 72.30 |

These noncompartmental PK parameters were derived from PTK/ZK plasma concentration data obtained on day 1 and day 28 from patients with colorectal cancer and liver mestastases, who received continuous once-daily PTK/ZK doses

and 28) achieved for each dose level are listed in Table 1. The PTK/ZK exposure achieved up to 1000 mg/day appears to be dose proportional, while the PTK/ZK exposures above 1000 mg/day appears to have reached a plateau. The result of fitting to an inhibitory $E_{max}$ model for the MRI IAUC to plasma AUC (exposure) and efficacy to plasma AUC (days 2 and 28) are shown in Fig. 2. The corresponding parameters for these fittings are listed in Table 2. An $EC_{50}$ for the MRI IAUC that was similar to the $EC_{50}$ for efficacy indicated that the MRI IAUC is likely a marker of biological activity.

*Legend: P = Progressors. NP = Non-Progressors. NE = Not Evaluable.*
*2 Patients with very high IAUC not shown on graph.

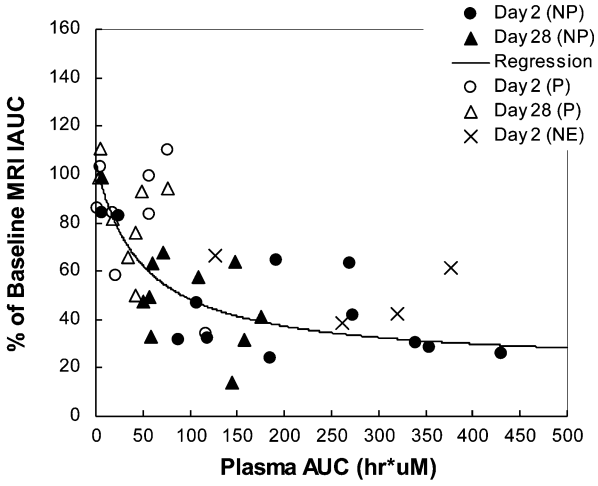


*Legend: P = Progressors. NP = Non-Progressors. NE = Not Evaluable.*
*Tumor measurement on day 28, if day 56 is not available.

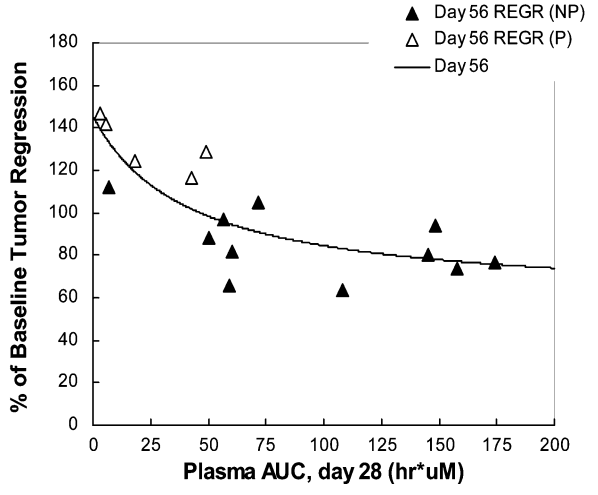


**Fig. 2** Man: exposure–response relationships as characterized by an inhibitory Emax Model. Top: % of Baseline IAUC versus PTK/ZK AUC. *2 patients with very high IAUC not shown on graph. In man, all available DCE-MRI of metastases and PTK/ZK plasma AUC data from day 2 and day 28 were fitted to an inhibitory Emax model to obtain $E_o$, $E_{AUC}$, and $E_{max}$. Bottom: % of baseline tumor regression versus PTK/ZK AUC. *Tumor measurement on day 28, if day 56 is not available. All available tumor size (day 56, liver metastases) and PTK/ZK plasma AUC (day 28) were also fitted to an inhibitory Emax model to obtain $E_o$, $E_{AUC}$, and $E_{max}$. Legend: *P* progressors, *NP* nonprogressors, *NE* not evaluable

**Table 2** Estimated inhibitory $E_{max}$ parameters (CV%) for plasma PTK/ZK AUC versus MRI IAUC and antitumor activity in man versus mouse

| | Man | | Mouse | |
|---|---|---|---|---|
| | MRI (% of baseline IAUC) | Efficacy (% of baseline tumor size) | MRI (% of baseline IAUC) | Efficacy (%T/C) |
| Eo | 104.9 (14.7) | 145.3 (10.2) | 98 (11.2) | 98.7 (14.9) |
| $E_{AUC50}$ | 48.4 (68.1) | 41.9 (97.3) | 69.8 (267) | 78.4 (213) |
| $E_{max}$ | 20.8 (52.8) | 22.7 (38.5) | 59.9 (68.9) | 35.8 (144.5) |

In man, all available DCE-MRI of metastases and PTK/ZK plasma AUC data from day 2 and day 28 were fitted to an inhibitory Emax model to obtain $E_o$, $E_{AUC}$, and $E_{max}$. All available tumor size (day 56, liver metastases) and PTK/ZK plasma AUC (day 28) were also fitted to an inhibitory Emax model to obtain $E_o$, $E_{AUC}$, and $E_{max}$

In mouse, all available MRI (day 3) and PTK/ZK plasma AUC (day 1, derived from dose) were fitted to an inhibitory Emax model to obtain $E_o$, $E_{AUC}$, and $E_{max}$. All available % T/C tumor size (day 7, metastases) and PTK/ZK AUC (day 1, obtained from dose) from day 28 were also fitted to an inhibitory Emax model to obtain $E_o$, $E_{AUC}$, and $E_{max}$

The MRI findings, supported by the efficacy data, suggests that most of the patients with "nonprogressive" disease achieved a PTK/ZK exposure of 50 h μM. At this exposure, the threshold MRI IAUC required for "nonprogressive" disease is approximately 60% of baseline IAUC (or 40% reduction in enhancement). This PTK/ZK exposure is achieved on day 28 with at least 1000 mg (562 mg/m$^2$) dose, where 50 h μM PTK/ZK exposure is approximately one standard deviation below mean exposure.

At 1000 mg dose and higher, a substantial rise in plasma VEGF and bFGF within 28 days of PTK/ZK

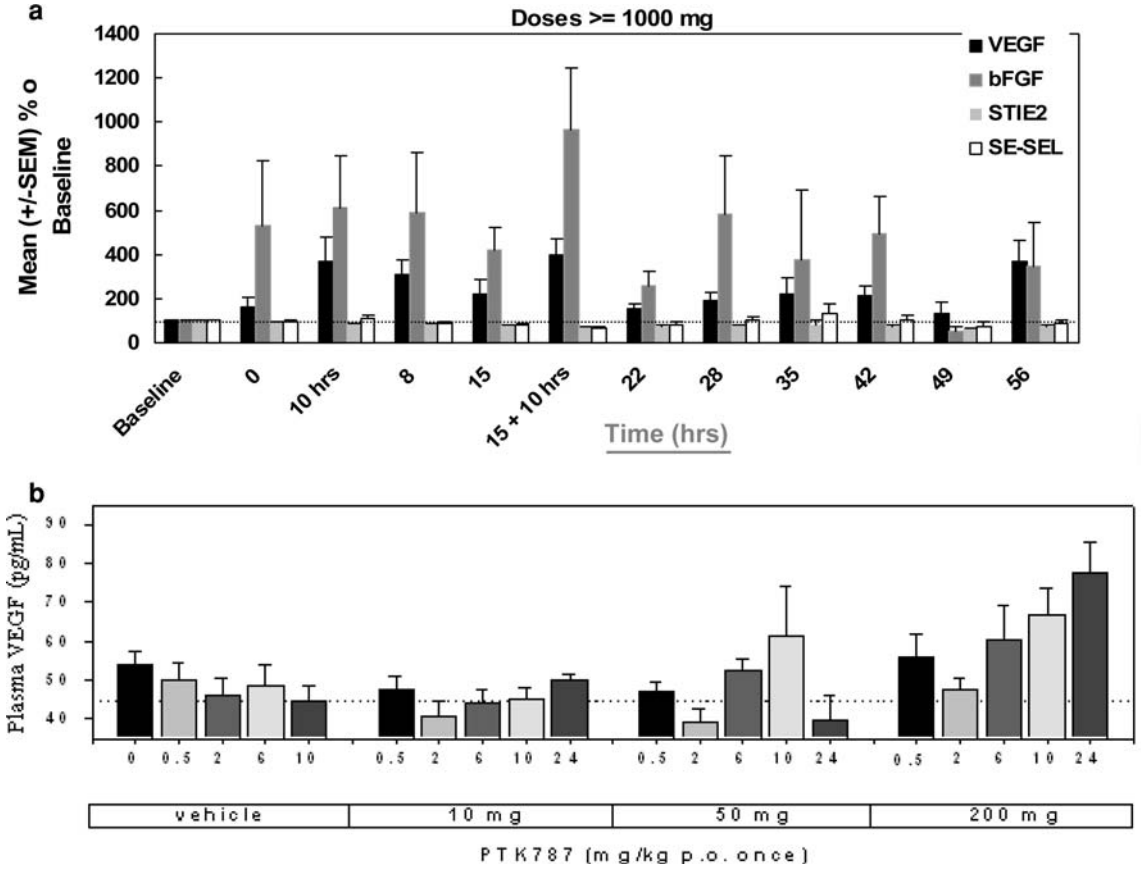


**Fig. 3** **a** Clinical: changes in % of baseline for soluble markers over 56 days of PTK/ZK treatment in patients who received at least 1000 mg dose. In man, this figure demonstrates a substantial increase in % change VEGF and bFGF from baseline for patients with colorectal cancer and liver metastases, receiving at least 1000 mg continuous once-daily PTK/ZK within the first 2 cycles of treatment (56 days). Below 1000 mg, % change in VEGF and bFGF was negligible and was not shown in the graph.**b** Preclinical: changes in plasma VEGF within 24 h of PTK/ZK treatment in mice (10, 50 and 200 mg/kg). In mouse, this figure also demonstrates the change in soluble markers from baseline, expressed in actual values. A significant rise in VEGF was observed at 50 mg (10 h), a dose with AUC that approximates at least 1000 mg dose

**Table 3** Mean ± (SD) plasma AUC PTK/ZK for mice after a single dose

| Dose (mg/kg/day) $N$ = (day 1) | Pharmacokinetic parameter $AUC_{0-\infty}$ (day 1) |
|---|---|
| 10 (4) | 5.95 ± 1.83 |
| 50 (3) | 62.42 ± 16.02 |
| 200 (3) | 238.66 + 27.31 |

These non-compartmental PK parameters were derived from PTK/ZK plasma concentration data obtained from B16/BL6 mice after a single PTK/ZK dose

treatment was observed as shown in Fig. 3a. At doses below 1000 mg, the change in plasma VEGF and bFGF was negligible.

## Preclinical studies

The dose-PTK/ZK exposure relationship is shown in Fig. 1 (bottom), and the PTK/ZK exposures achieved for each dose level are listed in Table 3. The result of fitting to the inhibitory $E_{max}$ model for the MRI-IAUC versus the dose of PTK/ZK and the efficacy versus the dose of PTK/ZK are shown in Fig. 4. The parameters for the fittings are listed in Table 3.

The combined MRI and efficacy result suggests that 50 mg/kg (170 mg/m$^2$) achieved the maximum results in terms of reduction in enhancement and reduction in tumor growth compared to control (Fig. 4). For the efficacy assessment, the results for 50 mg/kg was performed in a separate experiment and showed very similar %T/C to the 100 mg/kg dose (not shown in Fig. 4 bottom). The observed maximum efficacy on tumor growth achieved was an activity level of 36% T/C (64% reduction in tumor growth compared to control). In contrast, the observed mean maximum DCE-MRI effect achieved was 75–76% of baseline IAUC (or 25–24% reduction in enhancement) for the 100 and 50 mg/kg doses, respectively, which was statistically significant ($P \leq 0.032$) compared with baseline (2-tailed paired $t$test) as shown in Fig. 4 (top).

Vehicle or 10 mg/kg PTK787 treatment did not affect plasma VEGF levels over the 10 h posttreatment, but the efficacious doses (50–200 mg/kg) induced significant increases compared to baseline after 10 h (Fig. 3b) which was consistent with the clinical data described above for VEGF (Fig. 3a).

## Clinical–preclinical comparison and correlation

The result of the allometric scaling for the PK parameters (Cl, V) using three species (mouse, rat, dog) is shown in Fig. 5. Using the allometric equations with the fitted coefficient and exponent, the percent error for the predicted PK parameters were

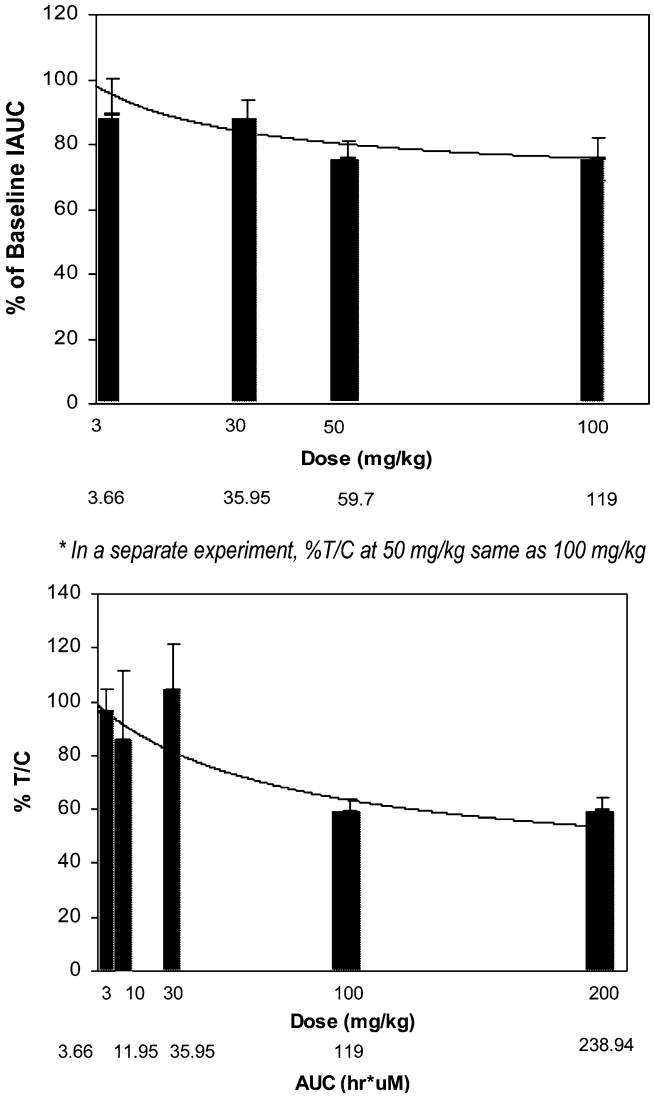


**Fig. 4** Mouse: exposure–response relationship. Top: % of baseline IAUC versus PTK/ZK AUC. In mouse, all available DCE-MRI of metastases (day 3) and PTK/ZK plasma AUC (day 1, derived from dose) were fitted to an inhibitory Emax model to obtain $E_o$, $E_{AUC}$, and $E_{max}$. Bottom: % of baseline tumor response versus PTK/ZK AUC. All available % T/C tumor size (day 7, metastases) and PTK/ZK plasma AUC (day 1, obtained from dose) from day 28 were also fitted to an inhibitory Emax model to obtain $E_o$, $E_{AUC}$, and $E_{max}$. * In a separate experiment, %T/C at 50 mg/kg was same as 100 mg/kg

39% (Cl/F) and 5% (V/F). The PK AUCs simulated in the clinical dose range of 50–2000 mg were generally overestimated; however, this should not impact the result since the MRI effects were simulated for a wide range of PK AUCs spanning from 0 to 500 h*μM. Accordingly, the PK AUCs should be used as an initial target surrogate for achieving the desired MRI effect in the clinical studies. Since the MRI effect is highly correlated to PK AUCs, they may represent the exposure achieved either after first dose or at steady state.

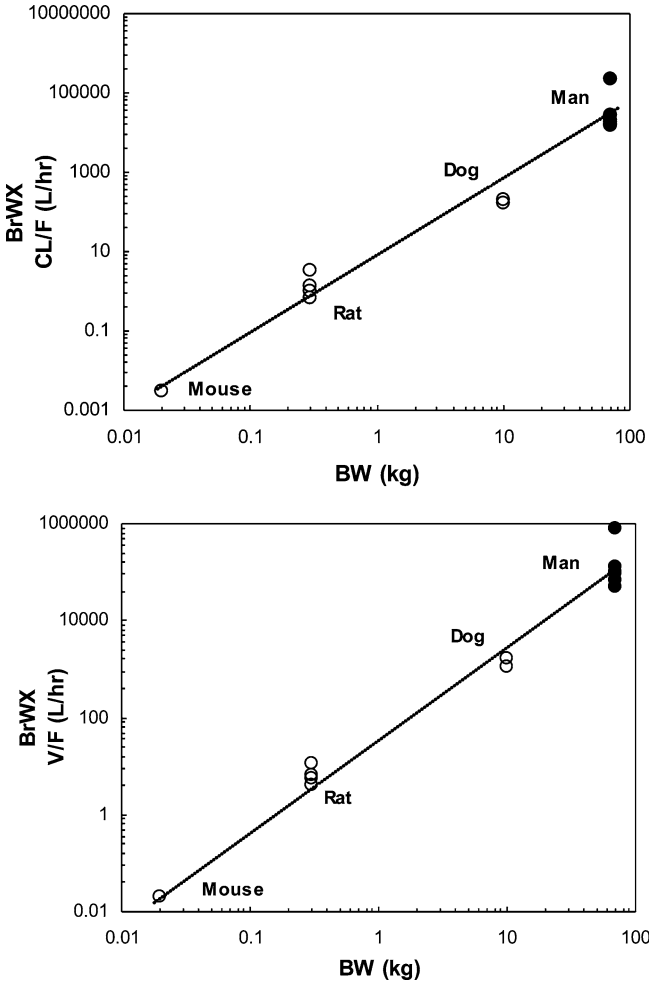


**Fig. 5** Allometric scaling for PK Parameters (Cl, V) using 3 species (mouse, rat, dog), and prediction of Cl and V in man. Top: allometric scaling (including brain weight) using fitted Cl/F parameter for mouse, rat and dog after a single PTK/ZK dose. Result show that predicted Cl/F in man lies within 95% CI of observed Cl/F in man on day 1. Bottom: allometric scaling (including brain weight) using fitted V/F parameter for mouse, rat and dog after a single PTK/ZK dose. Result show that predicted V/F in man lies within 95% CI of observed V/F in man on day 1

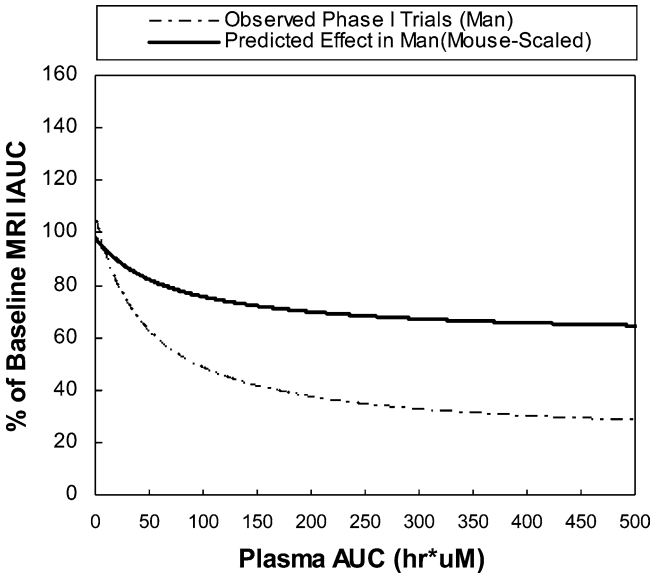


**Fig. 6** Predicted MRI effects in man (mouse-scaled) versus observed MRI effects in phase I trials. The *dotted line* depicts the fitted regression curve to observed DCE-MRI data from phase I studies (Fig. 2, top). The *dark line* represents the predicted MRI effect in human via simulation using scaled PK parameters and PD parameters obtained from preclinical species. This is a comparative figure demonstrating the differences and similarities in exposure-effect between the observed phase I data versus predicted human data based on preclinical data

The mouse PD parameter obtained from fitting the MRI IAUC effect were used in the prediction. The comparison between the predicted MRI effect in man, using scaled PK-PD parameters, versus the observed MRI effect is depicted in Fig. 6. An evaluation of the MR-IAUC effect curves suggests that the preclinical PK-PD data obtained from the B16/BL6 melanoma model can approximate the sensitivity of effect ($E_{AUC50}$: potency). However, the maximum effect ($E_0$: efficacy) was substantially lower in man compared to the B16/BL6 melanoma model. The differences in reduction of IAUC may be explained by the depiction in Fig. 7a, which indicates a strong trend for PTK/ZK (30–100 mg/kg) to increase blood flow in the B16/BL6 melanoma, while rBVol was unchanged (Fig. 7b). Since the GdDOTA contrast agent is influenced by flow as well as permeability, the increased blood flow would reduce the extent of the apparent decrease in the IAUC. This effect probably occurs to a lesser extent in patients due to the less chaotic nature of the tumor blood supply compared to the B16 which grow particularly fast; therefore, any 'normalization' of the tumor vasculature (see below) would be more dramatic in the mouse.

In retrospect, should the mouse exposure-effect data be available prior to start of clinical studies, the target exposure to aim for would be that which corresponded to the maximum MRI effect, i.e., at 50 mk/kg. In the mouse model, a single dose of 50 mg/kg achieves a PTK/ZK exposure of $62.42 \pm 16.02$ h*μM. The lower limit of standard deviation is 46.4 h*μM and this is comparable to the PTK/ZK exposure of 50 h*μM at the 1000 mg dose level in patients. Doses of 1000 mg and above were required for nonprogressive disease in the clinical studies and a dose of 1200 mg/day was chosen for further evaluation in the phase II/III PTK/ZK trials. Thus, the drug exposure required for the maximum MRI effect and antitumor activity in the mouse tumor model is similar to the drug exposure at clinically active doses for PTK/ZK in patients. Furthermore, the rise in plasma VEGF levels after 10 h in mice and man supports 1000 mg as the biologically active dose.

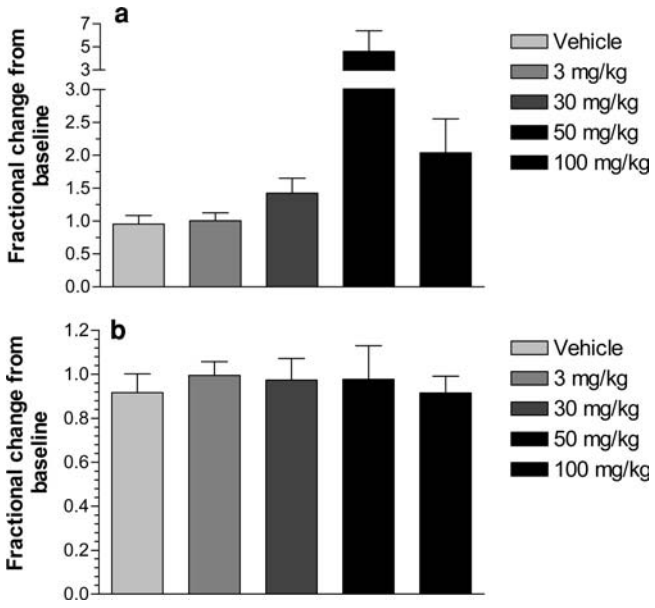


**Fig. 7** Effect of PTK787 on DCE-MRI measured blood-flow (**a**) and blood volume (**b**) in B16/BL6 lymph-node metastases. B16/BL6 lymph-node metastases were studied with DCE-MRI as described in Method using the intravascular contrast agent, Endorem, to determine **a** tumor blood flow (BFI) and **b** the relative tumor blood volume (rBVol). Tumors were studied both before treatment (baseline) and 3 days after daily treatment with vehicle or PTK/ZK at the different doses shown. Results show the mean ± SEM percentage change pooled from several different experiments for the different treatments of 0, 3, 30, 50 and 100 mg/kg PTK/ZK using 17, 8, 12, 4 and 12 mice, respectively

## Discussion

Comparatively, little research has been done to assess the validity and predictability of the animal models which are used to extrapolate to the clinical situation. In general, opinions differ considerably on the predictability of animal models [18, 19]. There are several potential limitations to approaches that attempt this validation, due in particular to differences in the pharmacokinetics of various drugs across species. In addition, differences in tumor genotypes, phenotypes, and microenvironment may contribute to variability in response. In spite of these limitations, animal models are necessary to select and profile new drugs. In this study, we analyzed whether the activity of the VEGFR tyrosine kinase inhibitor PTK/ZK in a mouse metastatic melanoma model correlated with response of liver metastases in patients with colorectal cancer from two phase I clinical trials. Evaluations were performed using radiological and soluble biomarkers such as DCE-MRI and plasma VEGF which, respectively, measures the change in tumor vascularity and biological tumor response to PTK/ZK treatment. Direct endpoints such as change in tumor size with PTK/ZK treatment were also compared in both animal and man. Earlier studies had already demonstrated that PTK/ZK treatment decreased tumor vascularity as measured by DCE-MRI [5, 6] and lead to a rise in plasma VEGF levels induced by tumor hypoxia [10], both of which were associated with antitumor activities in animals and clinical trials.

In this study, we have confirmed that a change from baseline in the MRI-measured IAUC for the B16/BL6 melanoma model after treatment with PTK/ZK appeared to correlate well with antitumor activity of the agent. Interestingly, the efficacy of the drug seemed to plateau at doses of 50 mg/kg, which may reflect that high concentrations (0.5 mM) are reached in the well-vascularized cervical lymph-nodes after a single dose [6]. We then attempted to study the pharmacokinetics–pharmacodynamic relationships in this mouse model and tried to correlate it with the clinical results observed in humans. Our data suggests that at drug plasma exposures above 50 h*μM (achieved at a dose of 50 mg/kg), maximal efficacy was achieved. Interestingly, similar drug exposures separated the 'progressors' from 'nonprogressors' in the human clinical trials of PTK/ZK. Thus, the mouse B16/BL6 melanoma model appeared to be predictive of both tumor response and the pharmacodynamic effects of PTK/ZK in patients at equivalent exposures. Furthermore, consistent with the clinical study, there was a rise in plasma VEGF after 10 h following treatment with PTK787, but only for the efficacious doses. It may be hypothesized that an increase in plasma VEGF level, a potent angiogenic cytokine, is explained by a feedback mechanism in which inhibition of new blood-vessel formation by PTK/ZK induces tumor hypoxia which in turn stimulates expression of HIF-1 and thus synthesis of more VEGF [20, 21]. This phenomena was observed in both the animal model and clinical studies at similar exposures of PTK/ZK.

There were several considerations in setting up this model system. The pharmacokinetic and pharmacodynamic measurements in the preclinical study were designed to mimic the clinical situation. The preclinical dose range spanned the entire range of PTK/ZK exposure achieved in the clinical studies. Since a variant form of CYP3A4 enzyme exists in mice and no enzyme induction was observed, PK sampling taken after the first dose was sufficient to represent clinical PTK/ZK exposure achieved at steady state. The tumor doubling time for mouse is 2–3 days [6], while the tumor doubling time for man, i.e., in this case liver metastases, is approximately 2 months [22]. Based on this estimate, preclinical tumor efficacy assessments after one week of treatment should represent the clinical tumor stage at the end of cycle 2. It should also be noted that %T/C was used in preclinical assessments of antitumor activity because tumors did not regress (tumor growth was instead delayed), and was the best representation of the clinical % of baseline tumor regression. Due to limitations in mouse size and blood volume, serial PK and PD measurements could not be made in the same animal and this was a source of data variability.

Even though the current experiments were designed to recapitulate the clinical situation, some limitations

are nevertheless likely. Metabolism patterns are known to be highly variable between species leading to differences in the rate of metabolism, levels of enzymes, and substrate specificity. In particular, the cytochrome P450 metabolizing enzymes consists of considerable variations in the primary amino acid sequence across species. Drugs and their metabolites are usually eliminated from the body via urine or bile, and yet the urinary excretion and the overall elimination of drugs depend on the nature of the drugs and species. In addition, differences in pharmacological effects may be due to differences in receptor sensitivity and distribution. Although minimal interspecies differences are known in basic biochemical and physiological functions, recent studies in cloned receptors and fresh human tissue have shown that differences in receptor sensitivity and distribution do exist across species. In isolated kinase assays, PTK/ZK is approximately sevenfold less active against the mouse receptor than against the equivalent human receptor [1] and is one likely explanation for differences in potency and efficacy between man and mouse.

Although major pharmacokinetic variables govern ultimate drug concentration at the target in tumors, we attempted to correlate pharmacokinetic exposures across species with pharmacodynamic markers that were studied and validated in the clinic. It appears that this approach can be valid although an imperfect correlation was obtained. This is best illustrated by the results in Fig. 6 where the difference in the shape of the regression is probably accounted for by differences in absorption, metabolism, and tumor heterogeneity across species. Furthermore, differences in the rate of tumor growth in mouse and man have to be considered. The more rapid growth of the mouse tumor model in comparison to patient tumors is likely to lead to decreases in tumor blood volume and flow as the tumor outgrows its blood supply, and treatment with an antiangiogenic such as PTK/ZK may actually normalize the tumor blood supply and lead to improved perfusion, as hypothesised by Jain [20]. This trend was observed in the mouse model, where the intravascular contrast agent showed PTK/ZK increased blood flow, and since the DCE-MRI GdDOTA measurement is sensitive to both permeability and flow, the effect on IAUC may be attenuated somewhat by the increase in blood flow.

Apart from PK, PD and physiological differences between species, the differences in preclinical and clinical methodologies for DCE-MRI may also account for variations in the measured effects. These would include the different MRI hardware and magnetic field strength (4.7T vs. 1.5T) and subsequent difference in imaging protocols. Nevertheless, despite all the potential differences between species, our data show that the mouse model gives data that is consistent with and predictive of the response in man and show that the plasma AUC for response in the mouse can be used to estimate the active plasma AUC for patients.

In this investigation, the use of the DCE-MRI in a preclinical tumor model was evaluated as a translational marker for predicting antiangiogenic activity in man. We have shown that the level of PTK/ZK exposure having a maximal DCE-MRI effect as demonstrated in the B16/BL6 melanoma model can be used to guide the clinical dose selection. Maximum tolerated dose cannot be used to select doses of antiangiogenic drugs since they have a much greater safety profile than conventional antitumor therapies. Therefore a biomarker such as DCE-MRI and/or plasma VEGF can aid the selection of a more appropriate clinical starting dose and an accelerated dose escalation scheme to expedite the choice of the clinically active dose. The transfer of such findings from mouse to man may not be exact because of the many interspecies differences in target sensitivity, drug metabolism, and tumor growth. Nevertheless, the current evaluation was successful in demonstrating the process in which preclinical models and biomarkers can be used to predict the biologically active dose in man.

## References


1. Wood J, Bold G, Buchdunger E, Cozens R, Ferrari S, Frei J, Hofmann F, Mestan J, Mett H, O'Reilly T, Persohn E, Rösel J, Schnell C, Stover D, Theuer A, Towbin H, Wenger F, Woods-Cook K, Menrad A, Siemeister G, Schirner M, Thierauch KH, Schneider M, Drevs J, Martiny-Baron G, Totzke F, Marme D (2000) PTK787/ZK 222584, a novel and potent inhibitor of VEGF receptor tyrosine kinases, impairs VEGF-induced responses and tumor growth after oral administration. Cancer Res 60:2178–2189
2. Bold G, Altmann KH, Frei J, Lang M, Manley P, Traxler P, Weitfeld B, Buchdunger E, Cozens R, Ferrari S, Furet P, Hofmann F, Martiny-Baron G, Mestan J, Roesel J, Sills M, Stover D, Acemoglu F, Boss E, Emmenegger R, Laesser L, Masso E, Roth R, Schlachter C, Vetterli W, Wyss D, Wood J (2000) New anilino-phthalazones as potent and orally well absorbed inhibitors of the VEGF receptor tyrosine kinase useful as antagonists of tumor driven angiogenesis. J Med Chem 43:2310–2323
3. Drevs J, Muller-Driver R, Wittig C, Fuxius S, Esser N, Hugenschmidt H, Konerding MA, Allegrini PR, Wood J, Hennig J, Unger C, Marme D (2002) PTK787/ZK 222584 a specific vascular endothelial growth factor-receptor tyrosine kinase inhibitor, affects the anatomy of the tumor vascular bed and the functional vascular properties as detected by dynamic enhanced magnetic resonance imaging. Cancer Res 62:4015–4022
4. Drevs J, Hofmann I, Hugenschmidt H, Wittig C, Madjar H, Muller M, Wood J, Martiny-Baron G, Unger C, Marme D (2002) Effects of PTK787/ZK 222584, a specific inhibitor of vascular endothelial growth factor receptor tyrosine kinases, on parimary tumor, metastases, vessel density, and blood flow in a murine renal cell carcinoma model. Cancer Res 60:4819–4824
5. Morgan B, Thomas AL, Drevs J, Hennig J, Buchert M, Jivan A, Horsfield MA, Mross K, Ball HA, Lee L, Mietlowski W, Fuxuis S, Unger C, O'Byrne K, Henry A, Cherryman GR, Laurent D, Dugan M, Marme D, Steward WP (2003) Dynamic contrast-enhanced magnetic resonance imaging as a biomarker for the pharmacological response of PTK787/ZK 222584, an inhibitor of the vascular endothelial growth factor receptor tyrosine kinases, in patients with advanced colorectal cancer and liver metastases: results from two phase I studies. J Clin Oncol 21:3955–3964

6. Rudin M, McSheehy PMJ, Allegrini PR, Rausch M, Baumann D, Becquet M, Brecht K, Brueggen J, Ferretti S, Schaeffer F, Schnell C, Wood J (2005) PTK787 / ZK222584, a tyrosine kinase inhibitor of vascular endothelial growth factor receptor, reduces uptake of the contrast agent GdDOTA by murine orthotopic B16/BL6 melanoma tumors and inhibits their growth in vivo. NMR Biomed 18:308–321
7. Evelhoch JL (1999) Key factors in the acquisition of contrast kinetic data for oncology. J Magn Reson Imaging 10:254–259
8. Evelhoch JL, LoRusso PM, He Z, DelProposto Z, Polin L, Corbett TH, Langmuir P, Wheeler C, Stone A, Leadbetter J, Ryan AJ, Blakey DC, Waterton JC (2004) Magnetic resonance imaging measurements of the response of murine and human tumors to the vascular-targeting agent ZD6126. Clin Cancer Res 10:3650–7
9. Green S, Weiss GR (1992) Southwest Oncology Group standard response criteria, endpoint definitions and toxicity criteria. Invest New Drugs 10:239–253
10. Drevs J, Zirrgiebel U, Schmidt-Gersbach CI, Mross K, Medinger M, Lee L, Pinheiro J, Wood J, Thomas AL, Unger C, Henry A, Steward WP, Laurent D, Lebwohl D, Dugan M, Marme D (2005) Soluble markers for the assessment of biological activity with PTK787/ZK 222584 (PTK/ZK), a vascular endothelial growth factor receptor (VEGFR) tyrosine kinase inhibitor in patients with advanced colorectal cancer from two phase I trials. Ann Oncol 16:558–565
11. Traxler P, Allegrini PR, Brandt R, Brueggen J, Cozens R, Fabbro D, Grosios K, Lane HA, McSheehy P, Mestan J, Meyer T, Tang C, Wartmann M, Wood J, Caravatti G (2004) AEE788: a dual family epidermal growth factor receptor/ErbB2 and vascular endothelial growth factor receptor tyrosine kinase inhibitor with antitumor and antiangiogenic activity. Cancer Res 64:4931–41
12. Nelder JA, Mead R (1995) A simplex method for function minimization. Comput J 7:308–313
13. Akaike H (1974) A new look at the statistical model identification. IEEE Trans Automat Control 19:716–723
14. Schwarz G (1978) Estimating the dimension of a model. Ann Stat 6:461–464
15. Mahmood I, Balian JD (1996) Interspecies scaling: predicting clearance of drugs in humans. Three different approaches. Xenobiotica 26:887–95
16. Mahmood I, Balian JD (1996) Interspecies scaling: a comparative study for the prediction of clearance and volume using two or more than two species. Life Sci 59:579–585
17. Chiou WL, Barve A (1998) Linear correlation of the fraction of oral dose absorbed of 64 drugs between humans and rats. Pharm Res 15:1792–5
18. Bibby MC (2004) Orthotopic models of cancer for preclinical drug evaluation: advantages and disadvantages. Eur J Cancer 40:852–857
19. Voskoglou-Nomikos T, Pater JL, Seymour L (2003) Clinical predictive value of the in vitro cell line, human xenograft, mouse allograft preclinical cancer models. Clin Cancer Res 9:4227–4239
20. Raghunand N, Gatenby RA, Gillies RJ (2003) Microenvironmental and cellular consequences of altered blood flow in tumours. Br J Radiol 76:S11–S22
21. Tannock IF, Hill Richard P (1998) The Basic Science of Oncology, 3rd edn. McGraw Hill, New York
22. Jain RK (2001) Normalising tumor vasculature with anti-angiogenic therapy: a new paradigm for combination therapy. Nat Med 7:685–93